Identification and dynamic characteristics of the defects responsible for the radiation enhancement of atomic mobility in concentrated α-AgZn alloys

M. Halbwachs and J. Hillairet

Centre d'Etudes Nucléaires de Grenoble, Département de Recherche Fondamentale, Section de Physique du Solide, 85 X, 38041 Grenoble Cedex, France

(Received 4 January 1978)

Strain-relaxation measurements were conducted in order to follow directly under flux the enhanced rate of the stress-induced ordering which occurs in a Ag–30-at.%-Zn alloy, as a result of electron irradiation. From the consideration of activation energies for the quasistationary and stationary states, the migration energies for the two types of elementary defects involved in the observed enhancements were measured to be 0.56 ± 0.02 and 0.94 ± 0.02 eV, respectively, for the faster- and the slower-moving species. Further, direct comparison, for specimens in the well-annealed or prequenched condition, of the buildup profiles until a stationary regime is reached, together with quench studies, enabled the unambiguous identification of the faster-moving defect in the irradiated alloy as the single vacancy.

I. INTRODUCTION

Much experimental effort has been directed in the past years towards the determination of the radiation-enhanced ordering rate in binary substitutional alloys. This effort was motivated both by obvious technical implications for the behavior of reactor materials and by more fundamental purposes. Although many data are available in the literature,[1-5] mainly for Cu- and Ag-base alloys, the results obtained concerning the properties of the elementary atomic defects and the ordering mechanisms involved are not conclusive. With the exception of Lam and Rothman,[6] all previous workers have assumed that the defect mobilities are analogous to those in pure metals and implicitly supposed that the migration energy of the interstitial is smaller than that of the vacancy. However, as was recently underlined,[7] no calculations of the relative energies of vacancy and interstitial migration in concentrated alloys exist at the present time. Further, comparisons of the measured activation energies with the vacancy migration energy were not direct since they were generally referred to the migration energies in the solvant metals, due to the lack of information about the binary alloys.

Most prior work was based on the use of electrical-resistivity measurements to follow the kinetics of the short-range ordering. For a more selective and sensitive determination of this parameter to be made, measurement of the stress-induced (Zener) ordering rate has been preferred in the present study. The corresponding experiments were performed directly under flux (i.e., continuously, at the temperature of the irradiation) so that the ordering rate was obtained at every instant of the irradiation. This type of study is shown to bring out all of the necessary information relevant to the nature and the mobility of the defect species which contribute to the radiation enhancement of atomic mobility and ordering rate. Application to a Ag–30-at.%-Zn alloy irradiated with 2.5-MeV electrons is reported. Ag-Zn was selected because the characteristics of the Zener relaxation and the thermal-vacancy parameters are well known.[8] In addition, radiation-enhanced short-range ordering has been studied by electrical-resistivity measurements in Ag–9-at.%-Zn,[9] and the self-interstitials were shown to have strong binding with the undersized Zn solute.[10] Finally, this same system was used recently to model the segregation of Zn in Ag under irradiation.[11-13]

In this paper, the results for both the quasistationary and the stationary enhanced-ordering rates are given. The relative mobilities of self-interstitials and vacancies together with their respective migration energies are inferred. Also, the specific role of the vacancies was determined by means of combined quench and irradiation experiments. A discussion of the properties of the self-interstitials is contained in the following paper.[14]

II. METHOD AND MATERIAL

The physical parameter which is used to gain the desired information is the rate at which directional order is established, as a result of an applied stress. It can be shown that the rate of this so-called Zener relaxation is related to the instantaneous concentrations c_j and mean rates ν_j^* at which atom-defect interchanges occur by[15]

$$\tau^{-1} = \sum_j \alpha_j c_j \nu_j^* , \tag{1}$$

where the α's are efficiency factors and

$$\nu_j^* = \nu_{0j}^* \exp(-E_j^*/kT) . \quad (2)$$

Effective jump rates ν^* are distinguished from defect mobilities ν to take into account the fact that not all atom jumps are equally efficient in producing directional order.

The experimental procedure is simple in concept. At appropriate times in the irradiation schedule, a change in the state of stress is applied to the specimen which is initially in elastic equilibrium and the resulting strain is measured as a function of time. The anelastic strain relaxation is then analyzed by methods described in the literature.[8] Three cases can occur: First, under equilibrium conditions, the anelastic response curve is entirely defined by three parameters, namely, the relaxation strength, the average relaxation rate, and the width of the distribution spectrum of relaxation rates. This spectrum, which arises from the dispersion in local environments and atom jump rates in the disordered solid solution, has been shown to obey, in the Ag-Zn alloys under consideration, a log-normal distribution.[8] The central quantity is the weighted mean relaxation rate of the normalized distribution of relaxation rates. It can be derived easily, together with the distribution width, from a single relaxation curve.[16] Second, in nonequilibrium conditions, the relaxation rate is determined by the delayed relaxational method.[8] The chief concern is to avoid the problem of a possible simultaneous variation of the mean relaxation rate and the distribution width as the relaxation proceeds. The solution consists to reestablish during every successive measurement cycle the same initial (fully relaxed) supersaturation state and to trigger the relaxation after variable delayed times. Berry and Orehotsky[8] have shown that the initial slope of a family of delayed relaxation curves is, within a given constant, equal to the average relaxation rate at the very moment selected to start the change of stress. Consequently, the proper kinetics for the evolution of the relaxation rate are derived from this procedure without any restriction on the spatial homogeneity of defects or on a possible variation of the distribution width. Third, if the evolution satisfies the conditions of an homogeneous defect distribution, as was verified for the case of the very low defect concentrations involved in the present experiments, then the local slope of any relaxation curve can be used to obtain the proper instantaneous ordering rate, paying due regard to the predetermined values of the distribution width.[17]

The starting material was an Ag-30-at.%-Zn alloy prepared by melting in a quartz tube under vacuum the required amounts of 99.9999% pure Cominco Ag and 99.99995% pure Zn supplied by the Laboratoire d'Electronique et de Traitement de l'Information du Centre d'Etudes Nucléaires de Grenoble. The specimens were strips 250 μm $\times$2 mm $\times$ 10 mm obtained by cold rolling. They were given a 5-day anneal at 700 °C under vacuum, followed by a slow cooling. This treatment produced a grain size larger than 0.2 mm and a low dislocation density. Then the specimens were mounted in an inverted torsion pendulum with negligible inertia and alternately loaded and unloaded in torsion. The anelastic strain response curve was followed by means of a photocell detection system, with a sensitivity of about 10^{-4} angular degree; that is, one part in ten thousand of the total anelastic displacement. Automatic data acquisition allowed a displacement measurement to be recorded every second.

The radiation study was done with the device working in line with a Van de Graaff accelerator, in a constant flux of 4×10^{10} or 4×10^{11} e^-/cm^2 sec. The corresponding defect production rates are extremely small [about 4×10^{-12} and 4×10^{-11} (displacements per atom)/sec, respectively]. Irradiation temperatures were between −70 and +140 °C, that is 0.2 to 0.4 of the melting temperature in Kelvin. The induced defect concentrations in dynamic equilibrium were of the order of 10^{-7} to 10^{-10} atom^{-1}. For the quenching experiments, the specimens were heated in situ and quenched by raising a water bath precooled to 0 °C, until immersion. The corresponding cooling was roughly linear, at a rate of about 500 °C/sec.

III. PHENOMENOLOGICAL BACKGROUND

A. General balance equations

The following equations which express the balance between the rate of production and the rate of elimination of radiation-produced defects are the equations most widely used to describe the dynamic equilibrium which is established in metals and alloys exposed to a bombardment by energetic particles[18,19]:

$$\frac{dc_v}{dt} = \sigma\epsilon\phi - \rho_v c_v \nu_v - Z c_i (c_v + c_{\mathrm{th}})(\nu_i + \nu_v) , \quad (3)$$

$$\frac{dc_i}{dt} = \sigma\epsilon\phi - \rho_i c_i \nu_i - Z c_i (c_v + c_{\mathrm{th}})(\nu_i + \nu_v) . \quad (4)$$

In these expressions, the production of freely migrating defects is due to flux ϕ, with efficiency equal to the product of the displacement cross section σ and the number ϵ of uncorrelated Frenkel pairs emitted by primary knock-on. Their annihilation is both by mutual recombination

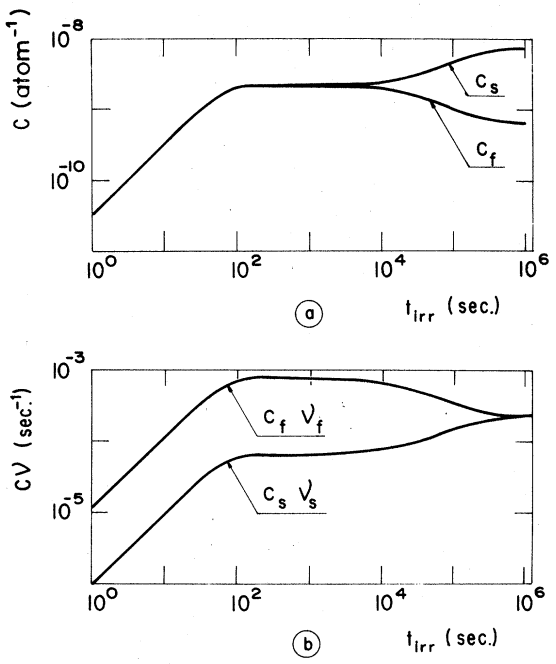

FIG. 1. Estimated buildup profiles expected for the defect concentrations and associated atomic mobility during an irradiation with a constant flux. Numerical values of $\nu_f^* = \nu_f = 2.5\times10^{14}$ exp (-0.55 [eV] /kT), $Z = 18$ and $\nu_s^* = \nu_s = 3.9\times10^{19}$ exp (-0.94 [eV] /kT), $\alpha_f = \alpha_s = 1$ were anticipated. Calculation was done for a temperature of 313 K and a defect production rate of 3.2×10^{-11}(displacements per atom) sec^{-1}, corresponding to a flux of roughly 4×10^{11} e^-/cm^2 sec. The sink density was 10^{-10} at^{-1}. It was assumed that freely migrating defects of either type, vacancy or self-interstitial, were produced in equal numbers, which is the case for electron irradiation.

characterized by a recombination factor Z, and by elimination at fixed sinks having a density ρ. In fact, ρ includes the efficiency of the sinks, which has to be distinguished for the two types of point defects; c_{th} is the thermal concentration of vacancies.

The numerical solution of these equations leads to the evolution of the defect concentrations versus time-of-irradiation profiles shown in Fig. 1(a). The newly introduced subscripts f and s in the figure denote, respectively, the faster- and the slower-moving species in the matrix, whichever they are. The physical meaning of the transient shape until a steady state is reached is as follows: During the first moments of the irradiation, the created defects are simply stored in the lattice, and this leads to a linear increase in their concentration. Then, due to the increased concentration levels, recombination events become significant, resulting in a curvature which is controlled by the recombination factor Z. This continues until a quasistationary level is reached, for which the concentrations of the two species are still equal. Progressively, the amount of faster-moving species being eliminated on dislocation sinks becomes no longer negligible, which results in a difference between the populations of the two species involved. The concentration of the faster-moving species is decreased while that of the slower species is increased, until a stationary state is completed for which the fluxes of both defects to dislocation sinks are equal; that is,

$$\rho_f c_f \nu_f|_{st} = \rho_s c_s \nu_s|_{st} . \tag{5}$$

Transposition of this scheme into mobility curves results in the pattern given in Fig. 1(b). The atomic mobility associated with the faster-moving species goes through a characteristic maximum before the curves for the two species join to satisfy the steady-state condition. Finally, the mean atom-jump frequency under irradiation is the sum of $c_f\nu_f$ and $c_s\nu_s$, and the measured Zener relaxation rate τ^{-1} is the weighted sum of these quantities, as indicated by expression (1).

Two cases are of special interest, for which the balance equations can be solved analytically. First, the mathematical treatment for the steady-state condition ($\partial c_v/\partial t = \partial c_i/\partial t = 0$) leads to stationary values for the defect concentration, which are

$$c_v = -\frac{1}{2}\left\{\left(\frac{\rho_i\nu_i}{Z(\nu_i+\nu_v)} + c_{th}\right) - \left[\left(\frac{\rho_i\nu_i}{Z(\nu_i+\nu_v)} + c_{th}\right)^2 + \frac{4\sigma\epsilon\phi}{Z}\frac{\rho_i}{\rho_v}\frac{\nu_i}{\nu_v(\nu_i+\nu_v)}\right]^{1/2}\right\}, \tag{6}$$

$$c_i = -\frac{1}{2}\left\{\left(\frac{\rho_v\nu_v}{Z(\nu_i+\nu_v)} + \frac{\rho_v\nu_v}{\rho_i\nu_i}c_{th}\right) - \left[\left(\frac{\rho_v\nu_v}{Z(\nu_i+\nu_v)} + \frac{\rho_v\nu_v}{\rho_i\nu_i}c_{th}\right)^2 + \frac{4\sigma\epsilon\phi}{Z}\frac{\rho_v}{\rho_i}\frac{\nu_v}{\nu_i(\nu_i+\nu_v)}\right]^{1/2}\right\}. \tag{7}$$

Hence, in the limiting conditions of low sink densities ($\rho \simeq 0$) and low temperatures ($\nu_s \ll \nu_f$), neglecting thermal vacancies against the radiation-produced vacancy concentration, the stationary rate can be written

$$\tau_{st}^{-1} = \left[\alpha_s\nu_s^*\left(\frac{\rho_f\nu_f}{\rho_s\nu_s}\right)^{1/2} + \alpha_f\nu_f^*\left(\frac{\rho_s\nu_s}{\rho_f\nu_f}\right)^{1/2}\right]\left(\frac{\sigma\epsilon\phi}{Z(\nu_s+\nu_f)}\right)^{1/2} \tag{8}$$

or, alternately, if one assumes $\nu^* \simeq \nu$,

$$\tau_{st}^{-1} \simeq (\alpha_s + \alpha_f)[(\sigma\epsilon\phi/Z)\nu_s]^{1/2}. \quad (9)$$

Second, with the above assumption of a low sink density the transient, until the quasistationary maximum corresponds, as a first approximation, to pure recombination ($\rho_i = \rho_v = 0$). Since $c_v = c_i$, the general balance equations condense into one single expression

$$\frac{dc}{dt} = \sigma\epsilon\phi - Zc^2(\nu_f + \nu_s), \quad (10)$$

whose integration leads to

$$c_v = c_i = [\sigma\epsilon\phi/Z(\nu_f + \nu_s)]^{1/2} \tanh(\sigma\epsilon\phi Z(\nu_f + \nu_s))^{1/2} t. \quad (11)$$

From this expression, it can be seen that c increases initially according to $dc/dt = \sigma\epsilon\phi$ and that it tends towards a quasistationary level $c_{qst} = [\sigma\epsilon\phi/Z(\nu_f + \nu_s)]^{1/2}$ for long times. Also, a characteristic time t^* can be defined, which corresponds to a fraction $(e-1)/(e+1) = 0.462$ of the asymptotic concentration. It is equal to

$$t^* = 1/[4\sigma\epsilon\phi Z(\nu_f + \nu_s)]^{1/2} \simeq 1/[4\sigma\epsilon\phi Z\nu_f]^{1/2}. \quad (12)$$

Transposition of these results to the rate curves leads to the following conclusions:

(i) If a maximum exists in the relaxation-rate versus time-of-irradiation curve, it demonstrates that the faster-moving species in the alloy brings a significant contribution to directional order. Since α_f is nonzero, the initial slope, as given by

$$\left.\frac{d\tau^{-1}}{dt}\right|_0 = (\alpha_f \nu_f^* + \alpha_s \nu_s^*)\sigma\epsilon\phi \simeq \alpha_f \sigma\epsilon\phi \nu_f^*, \quad (13)$$

is a measure of the mobility of the faster-moving species in the alloy. The maximum relaxation rate τ_{qst}^{-1} is directly related to the mobility of the fast defect by

$$\tau_{qst}^{-1} \simeq (\alpha_f \nu_f^* + \alpha_s \nu_s^*)[\sigma\epsilon\phi/Z(\nu_f + \nu_s)]^{1/2}, \quad (14)$$

that is, with the same assumptions as in (9),

$$\tau_{qst}^{-1} \simeq \alpha_f[(\sigma\epsilon\phi/Z)\nu_f]^{1/2}. \quad (15)$$

(ii) More generally, the mobility of the faster-moving species in the alloy, whether or not it participates in directional ordering, is provided by the characteristic time t^*, since this time does not depend on the efficiency factors α_f and α_s.

B. Predoping effects

This part is devoted to the special case when point defects, vacancies, or self-interstitials, have been selectively introduced into the crystal lattice prior to irradiation. The modifications to the radiation build-up profiles by the presence of these supplementary defects have to be analyzed. It is assumed that the preinjected defects have a low mobility at the temperature under consideration and are eliminated on dislocation sinks at a negligible rate. The irradiation condition is again one for which both species, vacancies and self-interstitials, are created and eliminated at parity. Their excess concentration, at every instant, is such that

$$\frac{dc}{dt} = \sigma\epsilon\phi - Zc(c + c_p)(\nu_s + \nu_f), \quad (16)$$

where c_p is the concentration of preinjected defects. Integration of this expression leads readily to

$$\ln\left|\frac{-c_p + [c_p^2 + 4\sigma\epsilon\phi/Z(\nu_s+\nu_f)]^{1/2}}{c_p + [c_p^2 + 4\sigma\epsilon\phi/Z(\nu_s+\nu_f)]^{1/2}} \frac{\frac{1}{2}\{c_p + [c_p^2 + 4\sigma\epsilon\phi/2(\nu_s+\nu_f)]^{1/2} + c\}}{\frac{1}{2}\{-c_p + [c_p^2 + 4\sigma\epsilon\phi/Z(\nu_s+\nu_f)]^{1/2} - c\}}\right| = Z(\nu_s+\nu_f)\left(c_p^2 + \frac{4\sigma\epsilon\phi}{Z(\nu_s+\nu_f)}\right)^{1/2} t. \quad (17)$$

It can be inferred that the transient curves upon irradiation should exhibit the same initial slope as in the undoped specimens, but different build-up times and modified quasistationary levels. More precisely, the characteristic times and quasistationary defect concentrations in excess of c_p for a predoped specimen, relative to the corresponding values in a nondoped condition, can be written, from expression (17),

$$\frac{t_p^*}{t_{p=0}^*} = \frac{2[\sigma\epsilon\phi Z(\nu_s+\nu_f)]^{1/2}}{Z(\nu_s+\nu_f)[c_p^2 + 4\sigma\epsilon\phi/Z(\nu_s+\nu_f)]^{1/2}} \quad (18)$$

and

$$\frac{c_{qst}|_p}{c_{qst}|_{p=0}} = \frac{-c_p + [c_p^2 + 4\sigma\epsilon\phi/Z(\nu_s+\nu_f)]^{1/2}}{2[\sigma\epsilon\phi/Z(\nu_s+\nu_f)]^{1/2}}. \quad (19)$$

(It is to be noted that, in the predoped condition, t^* corresponds to a fraction $(e-1)/(e-a)$ of the asymptotic level, where a is between 0 and 1 according to the concentration of preinjected defects.) Two experimentally attainable cases are of great interest; they deal with the predoping defects of the slower-moving species and the faster-moving species, respectively.

The predoping with the slower-moving defects can be achieved by suppression of the flux once

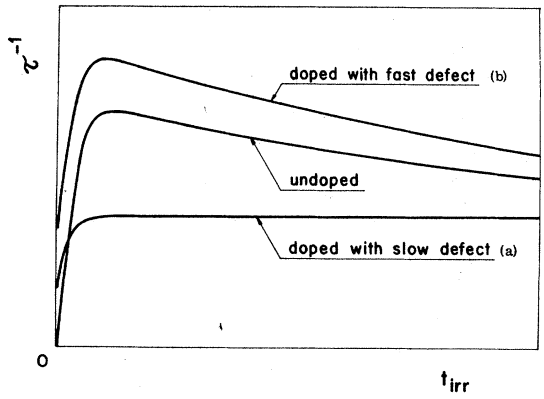

FIG. 2. Influence of predoping on the buildup profiles: (a) with defects of the slower-moving species (b) with defects of the faster-moving species. τ^{-1} is the relaxation rate.

a steady state has been established. Subsequently, the fast (minoritary) species anneals out rapidly by mutual encounter with the slow defects. Thus, after a suitable period, only the latter defects, which were the majority at steady state, still exist. A second irradiation run can then be triggered to study the way the remaining defects alter the pattern of the build-up curve. The mathematical treatment of this problem is given in the Appendix. The two major modifications which are expected are the decrease of the characteristic build-up time and the vanishing of the quasistationary maximum, as illustrated in Fig. 2.

If the preinjected defects, instead of being of the slow type, are the faster-moving ones, the above scheme is fundamentally altered. Qualitatively, it can be said that the extra-fast defects would just superimpose to the radiation-created (fast) ones, and bring an additive contribution to the ordering under flux. In particular, this is true for the initial part of the build-up curve, as it is controlled by the faster-moving species in the alloy. It can readily by verified in expressions (18) and (19) that if the concentration of preinjected defects is small against the quasi-stationary concentration, then

$$t_p^* \simeq t_{p=0}^*, \tag{20}$$

$$c_{qst}|_p \simeq c_{qst}|_{p=0}. \tag{21}$$

In other words, recalling that $c_{qst}|_p$ is the quasi-stationary concentration in excess of the predoping concentration, then the rate curve in the predoped condition is simply shifted upwards from that in the well-annealed state by c_p (Fig. 2), which is a very different situation from that expected for a predoping with slow defects. Since predoping with *vacancies* can be achieved with quenches, it is obvious that this type of experiment provides a selective tool to identify the faster-moving defect in the alloy.

IV. IRRADIATION RESULTS

It is clear that a number of kinetic parameters of each elementary defect can be collected if one is capable of following experimentally the evolution of the relaxation rate all along an irradiation run. Preliminary results have already been reported.[20] Figure 3 recalls the variation of the

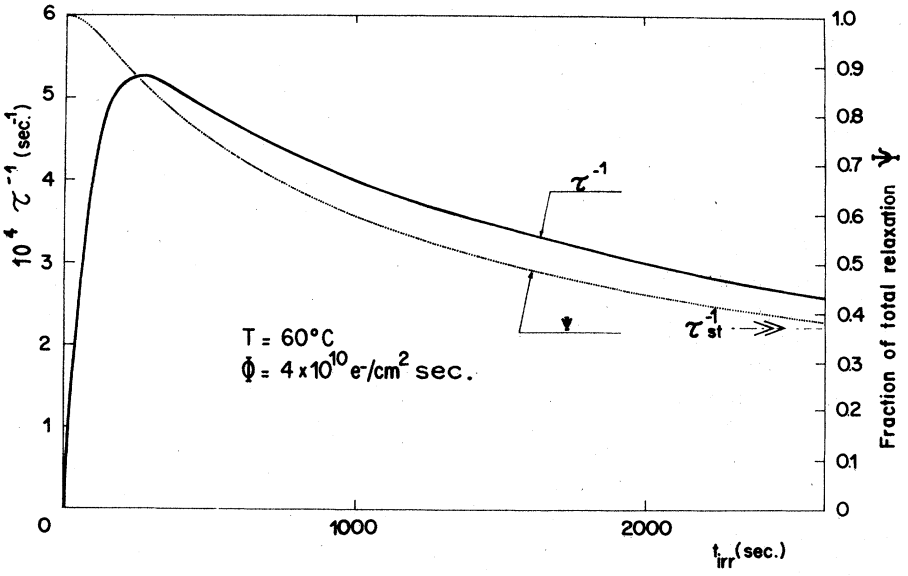

FIG. 3. Evolution of the relaxation rate with time of irradiation at 333 K in a constant flux of 4×10^{10} e^-/cm^2 sec. The fractional anelastic relaxation ψ is shown also (right-hand scale). The representation of both curves has been restricted to irradiation times up to 2600 sec. For longer times, only the asymptotic value is indicated, which was reached after 10^4 sec.

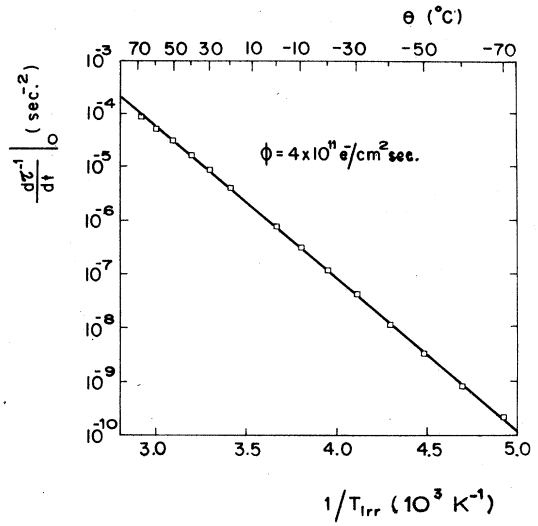

FIG. 4. Temperature dependence of the slope of the initial linear buildup of the rate curve, on application of a constant electron flux of $4\times10^{11}\ e^-/cm^2$ sec.

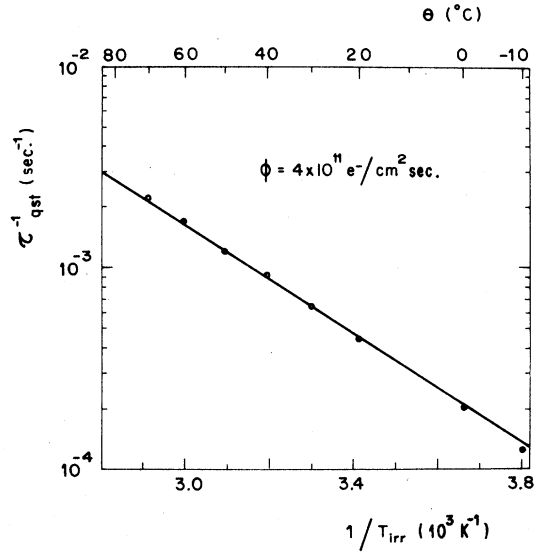

FIG. 5. Temperature dependence of the quasistationary relaxation rate, at a constant flux of $4\times10^{11}\ e^-/cm^2$ sec.

relaxation rate with time of irradiation which was observed on application of an electron flux. The rate curve at the measuring temperature of +60 °C exhibits an initial fast transient up to about 200 sec, followed by a slow decrease which extends over several hours, until a steady level is reached. Thus, its general shape is in agreement with the predictions of the models presented above. Further, a detailed comparison has shown that the transient up to the maximum obeys the analytical form given by expression (11) for the pure recombination case.[20]

The variations with temperature of the two parameters which define this part of the build-up curve, i.e., the initial slope and the quasistationary rate, have been studied in a constant flux of $4\times10^{11}e^-/cm^2$ sec. In Fig. 4 the measured initial slopes are shown in an Arrhenius plot. They have been determined over almost six orders of magnitude. Over the broad temperature range studied (i.e., −70–+70 °C) the data points are well represented by a straight line. An activation energy of 0.56± 0.02 eV is derived, which is the ordering energy E_f^* associated with the faster-moving species in the alloy. The same type of information was obtained independently by measurement of the temperature dependence of the quasistationary rate. This was done for temperatures ranging between −10 and +70 °C (Fig. 5). Again an activation energy of 0.56± 0.02 was found.

Turning to the stationary condition, Fig. 6 is an Arrhenius plot to show the variation of the stationary relaxation rate with temperature. A good linear fit was observed over the whole temperature range studied, between +40 and +140 °C, indicating a single activation energy of 0.47 eV. A value of 0.94± 0.02 eV is inferred for

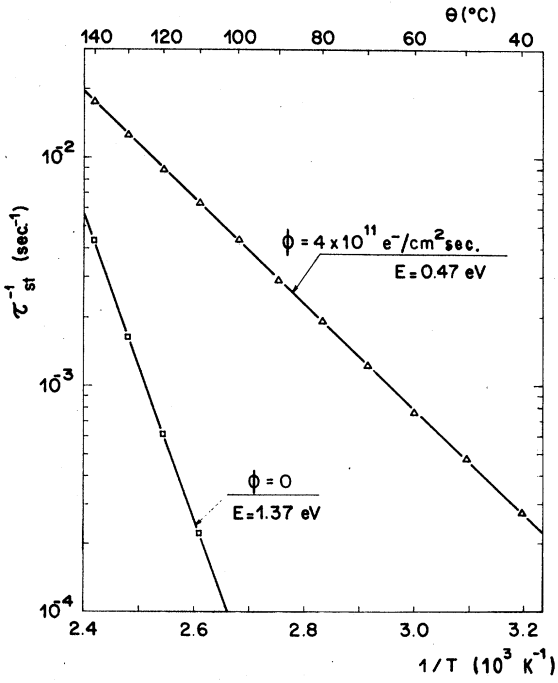

FIG. 6. Temperature dependence of the stationary relaxation rate, at the same flux of $4\times10^{11}\ e^-/cm^2$ sec. To show the radiation-induced enhancement factor, data points obtained in conditions of zero flux have been reported also.

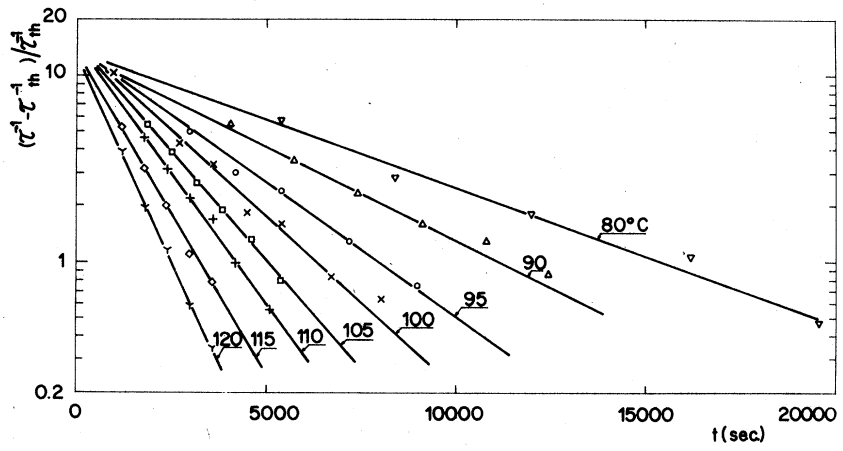

FIG. 7. Elimination kinetics of the quenched-in vacancy supersaturations, in a well-annealed specimen. First-order kinetics are obeyed. Each curve is labeled by the annealing temperature. The initial quench temperature was selected to result in a vacancy supersaturation of about 10.

the effective migration energy of the slower-moving species. Finally, it is to be noted that, using (8) and (12), comparison of the stationary and quasistationary enhancement levels leads to preexponential factors ν_{of} and ν_{os} which differ by five orders of magnitude. This result has been discussed in some detail elsewhere.[21]

V. QUENCH RESULTS

One of the specimens used in the present radiation work was given successive quenches from temperatures ranging between 145 and 210 °C, for which the equilibrium vacancy concentrations are 7.6×10^{-11} and 1.8×10^{-9} at. fractions, respectively.[8] After every quench, the temperature was rapidly raised up to the appropriate anneal temperature, i.e., between 80 and 120 °C.

The ratio of the relaxation rate after a quench and a further annealing treatment to the one at thermodynamical equilibrium at the same temperature is a direct measure of the vacancy supersaturation, as given by

$$(\tau^{-1}-\tau_{\rm th}^{-1})/\tau_{\rm th}^{-1}=(c_v-c_{v,\rm th})/c_{v,\rm th}=\Delta c_v/c_{v,\rm th}\,. \tag{22}$$

The kinetics for the elimination of this supersaturation are easily derived from the decrease of the relaxation rate during isothermal anneals, as measured by the initial slope method. Figure 7 is a semilog plot of the evolution with annealing time of this parameter. It can be seen that the kinetics are first order for all annealing temperatures, as expected for an elimination of single defects on fixed sinks. More precisely, the

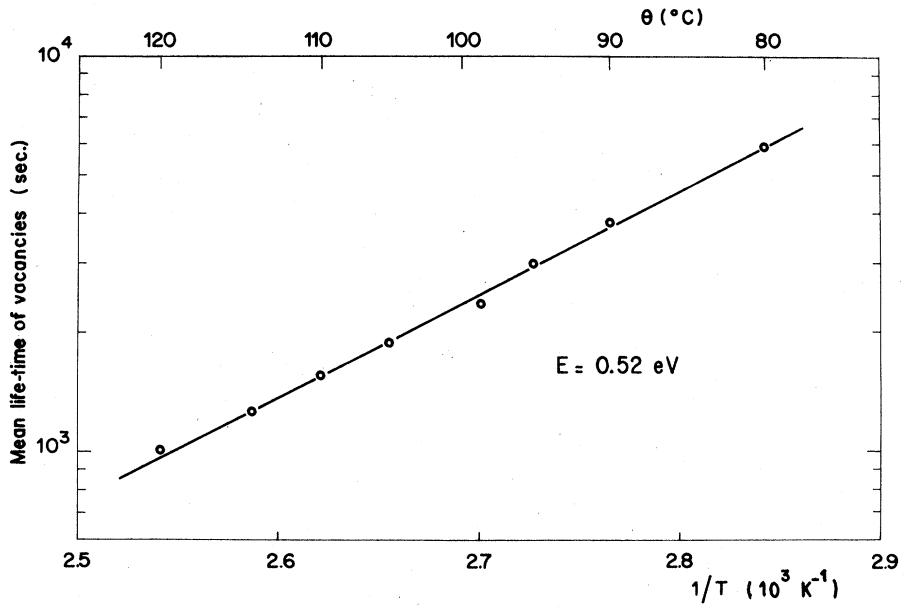

FIG. 8. Variation with anneal temperature of the characteristic decay time of the vacancy supersaturation induced by quenching.

relevant equation is written

$$c_v = c_v(0)\exp(-\rho\nu_v t), \tag{23}$$

where the characteristic time $(\rho\nu_v)^{-1}$ is simply the mean lifetime of vacancies. Hence, the associated activation energy is just the vacancy migration energy.

The measured temperature dependence of the decay time is shown in Fig. 8. It satisfies a Boltzmann variation, characterized by an activation energy of 0.52 eV. Prior work of Berry and Orehotsky[8] based on use of similar anelastic methods to study the elimination rate of the quenched-in vacancies in a Ag–24-at.%-Zn alloy had led to a similar value of 0.51 eV.

The sink density can also be estimated from these experiments. Assuming from the present work and Berry's data,[8] the mobility of vacancies to be

$$\nu_v = 2.5\times 10^{14}\exp[-0.52\ (\mathrm{eV})/kT], \tag{24}$$

a sink density of 5×10^{-11} atom^{-1} is derived. This rather low sink density is similar to that found by Berry,[8] i.e. 7×10^{-11} atom^{-1}, in well-annealed Ag–24-at.%-Zn alloys.

VI. PREDOPING RESULTS

First, the predictions of the predoping treatment have been verified for the case of the slow defects, at a temperature of 60 °C (Fig. 9). A first irradiation run was stopped after 2×10^4 sec in a flux of 4×10^{10} e^-/cm^2 sec. After a 4-h anneal at the same temperature, irradiation with same flux intensity was initiated again. Experimentally, the second irradiation profile exhibits good agreement with the theory, since the maximum is smoothed out and the stationary regime is attained faster than in the first irradiation run. These results provide a valuable check for the self-consistency of the two-defect model used to describe the dynamics of the defect populations which exist under electron irradiation.

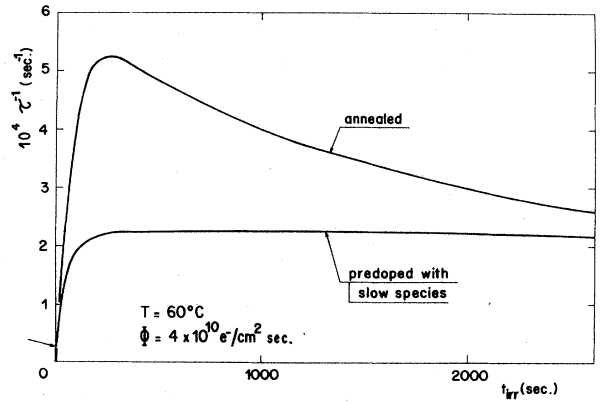

FIG. 9. Influence of a predoping with the slower-moving species on the pattern of the radiation buildup profile. The upper curve refers to a first irradiation run in the well-annealed condition (same as in Fig. 3). The lower curve corresponds to a second irradiation run conducted in the predoped condition. The arrow is to indicate the ordering rate at the start of the second irradiation run.

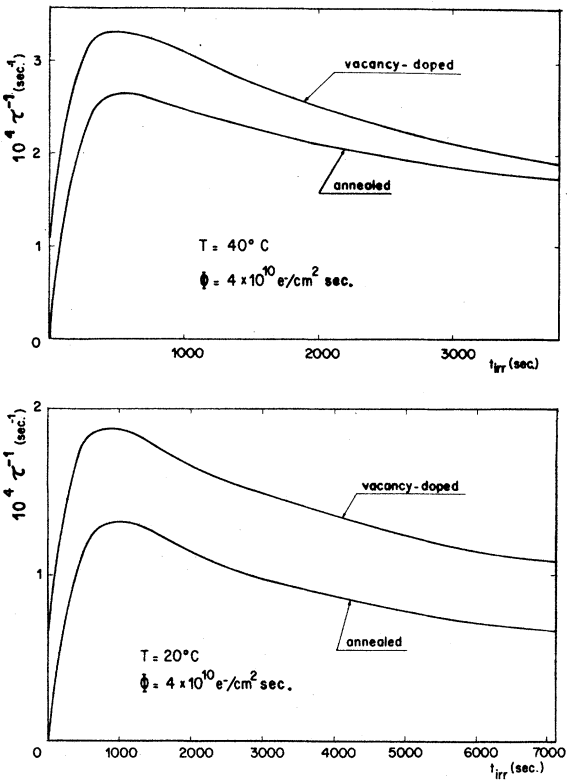

FIG. 10. Influence of a preliminary quench on the pattern of the radiation buildup profile. The 20 °C irradiation curve after quenching is simply shifted from the one in the undoped condition. For the 40 °C experiment the same effect is observed but the two curves tend to come closer to each other for long irradiation times. This trend is easily explained by the occurrence of a slight progressive annealing out of the quenched-in vacancies at sinks at this higher temperature.

In contrast, a specimen was quenched from 180 (or 200) to 0 °C, which resulted in the retention of a vacancy concentration of 5×10^{-10} atom^{-1} (or 1.2×10^{-9} atom^{-1}). It was then irradiated at 40 (or 20 °C). As shown in Fig. 10, the general pattern is exactly the same as that in the undoped condition. Clearly, the irradiation curves as traced after quenching are simply shifted from the normal ones along the rate scale. If one refers to the predictions of the general model

(Fig. 2), this result is a clear-cut demonstration that vacancy-type defects are responsible for the initial part of the build-up curve, the one controlled by the faster-moving species in the alloy.

VII. DISCUSSION

Complementary information about the properties of the faster-moving radiation defect—the vacancy—can be inferred from the consideration of the various parameters which characterize the irradiation curves.

(i) The characteristic time of about 100 sec at 60 °C which is found in Fig. 3 corresponds to a defect jump frequency of 10^7 sec^{-1}, as is readily derived from the analytical expression for t^*. In this calculation, the displacement cross section was taken equal to 100 b,[22] $\epsilon = 0.8$ and $Z = 18$.[17] Assuming the attempt frequency $\nu_{o,f}$ to be of the order of 10^{14} as is usual, an activation energy of roughly 0.5–0.6 eV is inferred. This supports identification of the vacancy as the faster-moving species, since the vacancy migration energy as measured after quenching is in this range.

(ii) From the temperature variation of the initial slope of the build-up radiation curve, as shown in Fig. 4, an activation energy of 0.56 eV is derived, that is the same as for vacancy migration. This means that the faster-moving species does contribute to the ordering process, which is consistent with the presence of a maximum. It is to be noted that the determination of this slope requires only a short measuring period, that is a very low number of defect jumps. Typically, at 20 °C, in a flux of 4×10^{11} e^-/cm^2 sec, only some 10 sec are needed, which means a number of defect jumps of the order of 10^6. The maximum defect concentration at the end of this period is $\sigma\epsilon\phi t = 3\times10^{-10}$. This shows that defect interactions with formation of dimers are highly improbable. Simultaneously, the observed good linearity for the build-up curve is a further indication that vacancy-interstitial interactions, which are equally probable, are insignificant. On the other hand, it is realized that most defects originally produced by the impinging 2.5-MeV electrons are single Frenkel pairs. Thus, it is clear that the measured activation energy of 0.56 eV for the initial slope refers to *single* vacancies.

(iii) A perturbation of the results by divacancies can be disregarded, for both quenching experiments and radiation work. After Berry and Orehotsky, the sum of formation and migration enthalpies for quenched-in thermal vacancies, as measured in a Ag–30-at.%-Zn alloy, is just the self-diffusion energy. The numerical values were, respectively, 0.84± 0.02 eV, 0.54± 0.02 eV, and 1.38± 0.02 eV. All three energies were obtained entirely by anelastic methods, which makes their comparison direct. Moreover, the mean number of elimination jumps was constant in the whole concentration range studied, that is 10^{-11} to 5×10^{-9} atom^{-1}. Further, in the present study, no curvature could be detected in the Arrhenius plot of the quasistationary rate under flux, although the vacancy concentrations varied between 10^{-9} and 2×10^{-8} atom^{-1}.

Now the relation between the vacancy jump frequency and the ordering rate has to be considered. The mobility of vacancies influences the ordering rate in two ways. First, it controls the lifetime of vacancies and hence their concentration under flux. In this respect, although the vacancy interchanges alternately with atoms of either type A or B of the constituant elements, the two types of jumps cannot be distinguished in the definition of the average migration rate of vacancies to sinks and the associated lifetime. The vacancy mobility ν_v is simply the sum $\nu_A + \nu_B$ of its interchange frequencies with atoms of type A and B. Hence, the vacancy migration energy is

$$E_v^M = \frac{\partial}{\partial(1/kT)} \ln\left(\frac{1}{\nu_A+\nu_B}\right). \tag{25}$$

On the other hand, the relation between these jump frequencies ν_A and ν_B and the resulting ordering rate is more complex. Clearly, not every atom jump does participate in the ordering. To evaluate the ordering rate, only A-B or B-A jumps are to be taken into account. A weighted frequency ν^* must be used, as defined by

$$2/\nu^* = K(1/\nu_A + 1/\nu_B), \tag{26}$$

where K is a constant.[23,24] Then the activation energy E^* associated with ν^* is

$$E^* = \frac{\partial}{\partial(1/kT)} \ln\left(\frac{1}{\nu_A}+\frac{1}{\nu_B}\right). \tag{27}$$

As a consequence, while the vacancy lifetime as measured in quenching experiments is determined by the faster jump, the ordering rate is controlled mainly by the slower jump.

Attention has been given to this problem in the alloy system under consideration. The frequencies ν_A and ν_B are related to the diffusion coefficients for the corresponding radioactive tracers by

$$D_A = c_v\nu_A a^2/C_A, \quad D_B = c_v\nu_B a^2/C_B, \tag{28}$$

where C_A and C_B are the atomic concentrations of constituants A and B. For the Ag-30-at.%-Zn solid solution, diffusion measurements between

500 and 700 °C lead to[25]

$$D_{Ag} = 0.29 \exp[-1.56\ (\mathrm{eV})/kT], \quad (29)$$

$$D_{Zn} = 0.46 \exp[-1.53\ (\mathrm{eV})/kT]. \quad (30)$$

Zn appears to diffuse faster than Ag, but the activation energies are very close, which indicates that E_v^* and E_v^M should not differ markedly. The discrepancy between the absolute values as determined by classical diffusion techniques and anelastic Zener measurements has been discussed in the literature.[15]

Along the same line, in a Ag–24-at. %–Zn alloy, Berry and Orehotsky[8] have measured $E_v^* = 0.56 \pm 0.02$ eV and $E_v^M = 0.51$ eV, with a lower accuracy. In the Ag–30-at. %–Zn, their result is $E_v^* = 0.54 \pm 0.02$ eV, while in the present work (i) from quenching experiments, $E_v^M = 0.52 \pm 0.04$ eV, (ii) from initial build-up rate, $E_v^* = 0.56 \pm 0.02$ eV, (iii) from quasistationary ordering rate, $2E_v^* - E_v^M = 0.56 \pm 0.02$ eV. All these variations are not significant. At any rate, it can be said that the difference between E_v^* and E_v^M, if it exists, is very small.

From the above considerations, one is led to conclude that the single vacancy has a higher mobility than the self-interstitial. In fact, the migration energy of the self-interstitial is 0.94 ± 0.02 eV, as is derived from the activation energy characteristic of the stationary regime (Fig. 6). On the other hand, comparison of the quasistationary and stationary enhancement levels, using (9) and (15), leads to a preexponential factor ν_{oi} which is five orders of magnitude larger than ν_{ov}. However, it is noted that this latter result was obtained assuming that ρ_i equaled ρ_v. This point together with the other parameters, such as α_i and α_v, which define the relative contributions of the self-interstitials and the vacancies to short-range ordering, will be discussed in more detail in the following paper.

VIII. SUMMARY

Experimental evidence has been presented that the single vacancy is the faster-moving species, in a Ag–30-at. %–Zn alloy exposed to electron irradiation. This defect was shown to control the initial transient of the enhanced ordering rate on application of an electron flux. Further analysis is needed to understand the physical reasons why the self-interstitial is slowed down. Much technological and theoretical interest is attached to this phenomenon. Of particular interest would be the study of the extent to which the observed inversion of defect mobilities extrapolates to lower concentrations in the Ag-Zn system and whether it applies as well to other alloy systems.

APPENDIX

The purpose of this Appendix is to evaluate the influence of a selective predoping with the slower-moving species on the build-up profile of an irradiation curve. As was explained in the text, this treatment can be achieved by suppression of the flux once a stationary regime has been obtained, followed by a controlled anneal to eliminate the faster-moving defects. Since the stationary concentration of these fast defects is much lower than that of the slow defects (Fig. 1), only the latter defects remain and in an almost unaffected number. Their concentration c_p is given by

$$c_p = c_{s,st} \simeq [(\rho_f/\rho_s)(\sigma\epsilon\phi/Z\nu_s)]^{1/2}. \quad (A1)$$

The irradiation profile for a predoped specimen is defined by the characteristic time of the initial build-up rise, the quasistationary level, and the final stationary level. Obviously, the final stationary concentration is not influenced by the predoping, since the preinjected defects are annealed out at sinks after a finite period of time and consequently their contribution vanishes.

The quasistationary concentration in the predoped condition is obtained by introducing expression (A1) in expression (16). One obtains

$$c_{f,qst} = \frac{1}{2}\left[-\left(\frac{\rho_f}{\rho_s}\frac{\sigma\epsilon\phi}{Z\nu_s}\right)^{1/2} + \left(\frac{\rho_f}{\rho_s}\frac{\sigma\epsilon\phi}{Z\nu_s} + \frac{4\sigma\epsilon\phi}{Z\nu_f}\right)^{1/2}\right]. \quad (A2)$$

Hence, assuming $\rho_s\nu_s$ to be smaller than $\rho_f\nu_f$ leads to

$$c_{f,qst} \simeq [(\rho_s/\rho_f)(\sigma\epsilon\phi\nu_s/Z\nu_f^2)]^{1/2}, \quad (A3)$$

that is, the quasistationary concentration for the fast species is equal, in the predoped specimen, to the stationary concentration. As a result, with the assumption that $\nu_f^* = \nu_f$ and $\nu_s^* = \nu_s$, the ratio of the quasistationary and stationary rates is

$$\frac{\tau_{qst}^{-1}|_p}{\tau_{st}^{-1}|_{p=0}} = \frac{\alpha_f[(\rho_s/\rho_f)(\sigma\epsilon\phi/Z)\nu_s]^{1/2}}{[\alpha_s + \alpha_f(\rho_s/\rho_f)][(\rho_f/\rho_s)(\sigma\epsilon\phi/Z)\nu_s]^{1/2}}. \quad (A4)$$

Assuming $\alpha_s\rho_f \ll \alpha_f\rho_s$ (Ref. 14) gives

$$\tau_{qst}^{-1}|_p \simeq \tau_{st}^{-1}|_{p=0}. \quad (A5)$$

The characteristic time t_p^* can be written

$$t_p^* = \frac{2}{[(\rho_f\nu_f/\rho_s\nu_s) + 4]^{1/2}} t_{p=0}^*. \quad (A6)$$

It is shorter than in the undoped condition.

The resulting profile is given in Fig. 2. The most striking modification of the radiation curve due to the predoping is the suppression of the quasistationary maximum.

[1]W. Schüle, P. Spindler, and E. Lang, Z. Metallk. 66, 50 (1975).
[2]G. Oleownik, W. Schüle, International Conference on Fundamental Aspects of Radiation Damage in Metals, Gatlinburg, Tennessee, 1975, edited by M. T. Robinson, and F. W. Young (unpublished), p. 341.
[3]K. Salomon, W. Schüle, Radiat. Eff. 16, 45 (1972).
[4]L. N. Bystrov, L. I. Ivanov, and Yu. M. Platov, Phys. Status Solidi A 7, 617 (1971); 8, 375 (1971).
[5]W. Schüle, E. Lang, P. Donner, and H. Penkuhn, Radiat. Eff. 2, 151 (1970).
[6]N. Q. Lam and S. J. Rothman, Phys. Status Solidi A 35, K13 (1976).
[7]A. C. Damask, J. Gilbert, and H. Herman, Radiat. Eff. 26, 89 (1975).
[8]B. S. Berry and J. L. Orehotsky, Acta Metall. 16, 683 and 697 (1968).
[9]L. N. Bystrov, L. I. Ivanov, and Yu. M. Platov, Phys. Status Solidi A 7, 617 (1971); 8, 375 (1971).
[10]Yu. M. Platov, M. N. Pletnev, V. I. Popov, and S. I. O. Sadykhov, Fiz. Met. Metalloved. 39, 1290 (1975).
[11]N. Q. Lam and R. A. Johnson, Nucl. Instrum. Methods 20, 121 (1976).
[12]R. A. Johnson and N. Q. Lam, Phys. Rev. B 13, 10 (1976).
[13]R. A. Johnson and N. Q. Lam, J. Nucl. Mater. 69—70, 424 (1978).
[14]M. Halbwachs, J. T. Stanley, and J. Hillairet, following paper, Phys. Rev. B 18, 4938 (1978).
[15]A. S. Nowick and B. S. Berry, *Inelastic Relaxation in Crystalline Solids* (Academic, New York, 1972), p. 238.
[16]A. S. Nowick and B. S. Berry, IBM J. Res. Dev. 5, 297; 312 (1961).
[17]M. Halbwachs, thesis (Université de Grenoble, 1977) (unpublished).
[18]G. J. Dienes and A. C. Damask, J. Appl. Phys. 29, 1713 (1958).
[19]W. M. Lomer, U. K. At. Energy Auth., AERE Report No. T/R-1540, 1954 (unpublished).
[20]M. Halbwachs and J. Hillairet, in Ref. 13, p. 776.
[21]M. Halbwachs, Phys. Status Solidi A 42, 707 (1977).
[22]O. S. Oen, U.S. AEC, ORNL, Report No. 4897, 1973 (unpublished).
[23]S. Radelaar, Proceedings of the International Conference on Vacancies and Interstitials in Metals, Jülich, Germany, 1968, edited by A. Seeger, D. Schumacher, W. Schilling, and J. Diehl (unpublished), p. 667.
[24]A. Caplain and W. Chambron, Acta Metall. 25, 1001 (1977).
[25]D. Lazarus and C. T. Tomizuka, Phys. Rev. 103, 5, 1155 (1956).